Biochemical and structural characterization of the flavodoxin-like domain of the *Schizosaccharomyces japonicus* putative tRNA[Phe] 4-demethylwyosine synthase Tyw1 in complex with FMN

Ljiljana Sjekloća[1,2§], Adrian R. Ferré-D'Amaré[1]

[1]Biochemistry and Biophysics Center, National Heart, Lung and Blood Institute, 50 South Drive, Bethesda, Maryland, 20892-8012, United States

[2]Current affiliation: Molecular Pathology, International Centre for Genetic Engineering and Biotechnology, Padriciano 99, Trieste 34149, Italy

[§]To whom correspondence should be addressed: ljsjeklo@gmail.com

Abstract

The S-adenosyl-L-methionine-dependent tRNA 4-demethylwyosine synthase TYW1 catalyzes biosynthesis of 4-demethylwyosine (imG-14), the precursor for wyosine, the hypermodified guanine-derived nucleotide present at position 37 of phenylalanine tRNAs of archaea and eukarya. Eukaryotic TYW1 enzymes contain N-terminal flavodoxin-like and C-terminal radical-SAM domains. We determined co-crystal structures of the flavodoxin-like domain of the putative Tyw1 from *Schizosaccharomyces japonicus* in complex with flavin mononucleotide (FMN), exploiting an unexpected anomalous scatterer present in the recombinant protein. Our results show how eukaryotic TYW1 enzymes bind the coenzyme FMN and will help further elucidation of the structural enzymology of 4-demethylwyosine synthesis.
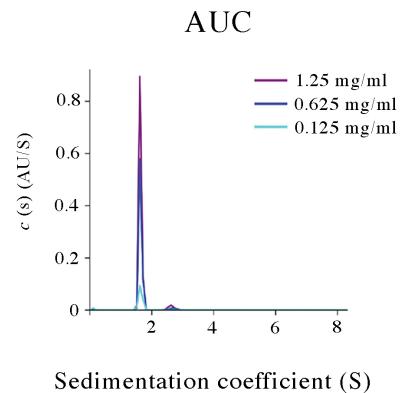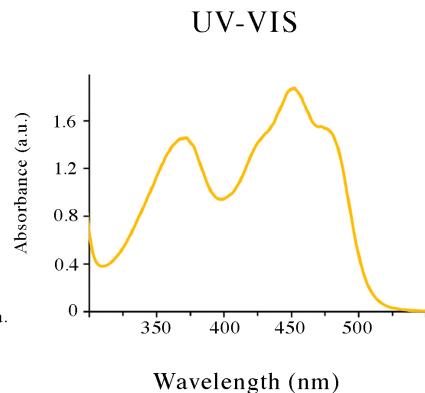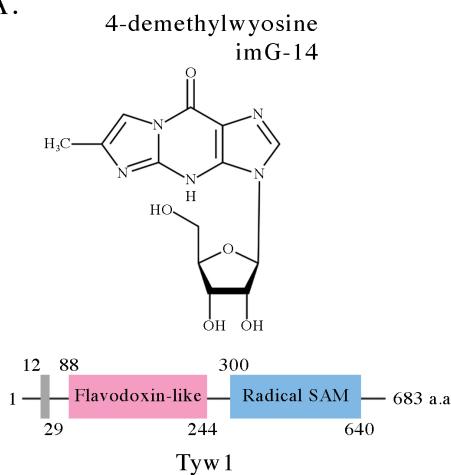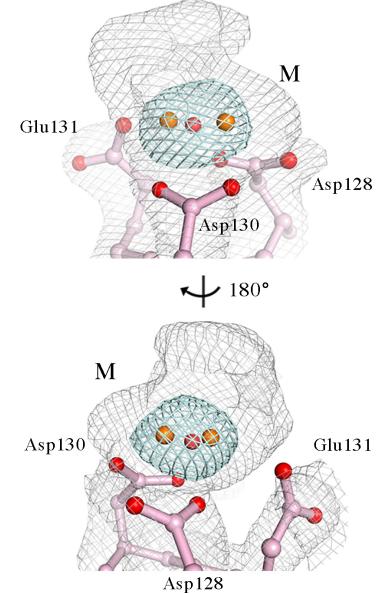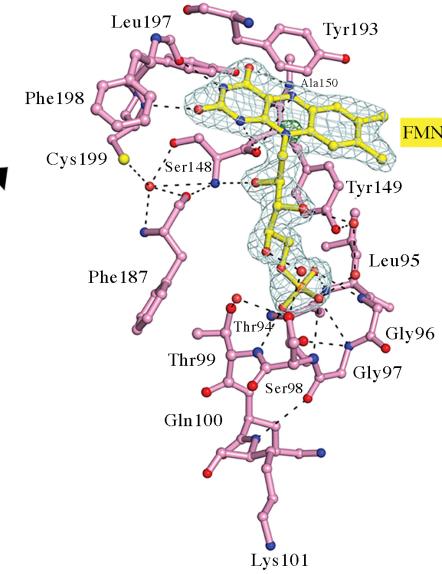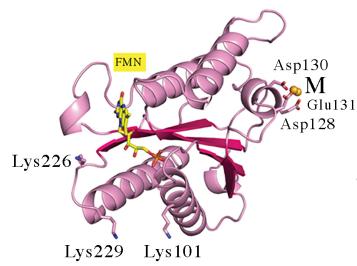
Figure 1. Biochemical and structural characterization of fungal Tyw1 flavodoxin-like domain:

A. Chemical structure of 4-demethylwyosine (imG-14) and predicted domain organization of *S. japonicus* Tyw1 (grey-membrane localization sequence, pink- flavodoxin-like domain, blue- radical SAM domain); UV-VIS spectrum of purified Tyw1 76-251 in the oxidized FMN-bound form, and *c*(S) distributions derived from velocity analytical ultracentrifugation (AUC) of Tyw1 30-251, consistent with a ~23.5 kDa protein domain, in close agreement with the calculated and mass-spectrometry-derived molecular masses (24940 Da and 25010 Da, respectively). **B.** Left: cartoon representation of the crystal structure of Tyw1 76-251 with the side chains of Asp128, Asp130 and Glu131 involved in metal (M) binding, and of Lys101, Lys226 and Lys229 close to the bound FMN in stick representation, and electrostatic potential mapped onto the molecular surface of Tyw1 76-251 in the same orientation. Center: the blown-up of the FMN binding site rotated ~ 90° counterclockwise around the vertical axis, respective to the orientation shown on the left; FMN is in ball-and-stick representation, gray mesh represents |Fo| - |Fc| electron density map (contoured at 3 standard deviations above mean peak height, 3 σ) before the FMN was built in the model. After the final refinement of the model there is only a minor residual electron density around isoalloxazine nitrogen N10; residues contacting FMN (pink) and hydrogen bonds (black dashed lines), and selected water molecules (red spheres) are shown. Right: two views rotated ~180°clockwise of the portions of $2|F_o| - |F_c|$ (gray mesh, 1 σ) and anomalous difference Fourier syntheses (cyan mesh, 7 σ), near Asp128, Asp130 and Glu131 (ball-and-stick representation). The crystallographic model (PDB 6PUP) contains two Mn (II) ions bridged by a water molecule (orange and red spheres, respectively).

Description

Wyosine (Y) (3-[(2*R*,3*R*,4*S*,5*R*)-3,4-dihydroxy-5-(hydroxymethyl)oxolan-2-yl]-4,6-dimethylimidazo[1,2-a]purin-9-one) is a tricyclic fluorescent nucleoside introduced into archaeal and eukaryotic phenylalanine tRNA through sequential enzymatic reactions targeting G37, immediately 3' to the anticodon. In the archaeon *Methanocaldococcus jannaschii*, wyosine synthesis starts with N^1-methylation of G37 by the methyltransferase TRM5 (Drogmans and Grosjean, 1987; Bjork *et al.*, 2001). Condensation of the resulting m^1G with pyruvate to form the tricyclic base 4-demethylwyosine imG-14 (Figure 1A) is catalyzed by the single-domain tRNA[Phe] 4-demethylwyosine synthase TYW1/TAW1, a member of the S-adenosine L-methionine (AdoMet) radical enzyme superfamily, which uses a 4Fe-4S cluster to reductively cleave SAM and activate pyruvate (Young and Bandarian, 2011; Young and Bandarian, 2015; Grell *et al.*, 2018). 4-demethylwyosine is the precursor to several wyosine derivatives detected by mass spectroscopic analysis and its hyper-modification by enzymes TYW3 and TYW4 lead to formation of wybutosine (yW) (Kasai *et al.*, 1976; Noma et al., 2006). Eukaryotic TYW1 are predicted, based on their sequences, to be multidomain, endoplasmic reticulum membrane-associated proteins (Figure 1 A Left). The best studied ortholog, *Saccharomyces cerevisiae* TYW1, comprises a membrane-spanning region followed by cytoplasmic flavodoxin-like and radical-SAM domains (Huh *et al.*, 2003; Waas *et al.*, 2005; Noma *et al.*, 2006; Li *et al*, 2011). Wyosine and its derivatives may modulate translation efficiency by tuning the affinity of tRNA[Phe] for phenylalanyl-tRNA synthetase (Krauss *et al.*, 1976) and by selectively preventing frameshifting (Hatfiled *et al.*, 1989; Noma *et al.*, 2006; Helm and Alfonzo, 2014). The *S. cerevisiae* Δ*tyw1* strain shows no phenotypic changes. However, reduced growth resulting from deletion of the iron importer protein gene *CCC1* can be overcome by TYW1 overexpression, suggesting TYW1 involvement in regulation of cytoplasmic free iron (Li *et al.*, 2011).

As an initial step in elucidating the role of flavin mononucleotide FMN in wyosine biosynthesis, we determined crystal structures at 1.5 Å and 1.9 Å-resolution of the flavodoxin-like domain of the putative *Schizosaccharomyces japonicus* Tyw1 in complex with FMN. *S. japonicus* Tyw1 recombinant fragments 30-251 and 76-251 were expressed in aerobically grown *E. coli*. The purified proteins are monomeric, and their intense yellow color and UV-VIS spectra are consistent with the presence of oxidized flavin mononucleotide $FMN_{(ox)}$ (Figure 1A Center). Diffraction data from Tyw1 76-251 crystals collected using 1 Å X-radiation extended to 1.9 Å resolution. Data analysis revealed anomalous signal, which was employed for structure determination by the single-wavelength anomalous dispersion (SAD) method (PDB 6PUP). Diffraction data from Tyw1 30-251 crystals collected using 1.1 Å X-radiation extended to 1.5 Å resolution and did not exhibit anomalous signal. This structure (PDB 6PUQ) was solved by molecular replacement using the Tyw1 76-251 structure (PDB 6PUP) as a search model. In the 6PUQ structure, there was no electron density corresponding to residues 30-80, suggesting disorder.

Tyw1 residues 81-250 adopt a Rossman-like fold comprised of a parallel, 5-stranded β-sheet flanked by α-helices, two on each side (Figure 1B Left, Extended Data Figure 1). The β-strand connectivity (2, 1, 3, 4, 5) is typical of flavodoxins, and the last strand (β5) does not contain an insertion (Extended Data Figure 2). Hence Tyw1 81-250 is a short-chain, flavodoxin-like domain (Drennan *et al.*, 1999). Loops at the N-terminal ends of the β-strands create a binding site for a single FMN molecule (Figure 1B Center). The isoalloxazine is in a planar conformation (Figure 1B Center). The pyrimidine ring hydrogen bonds with the backbone Cys199 and Leu197. The phenilenediamine ring forms polar contacts with the Ser148 carbonyl; this ring is shielded from solvent on its *si* face by Tyr149 and on *re* face by Tyr193 with which it makes π-π stack. The dimethylbenzene ring is the only solvent-exposed portion of the isoalloxazine. The ribityl oxygens are hydrogen-bonded to the Ser148 amide, and to two water molecules which in turn H-bond with Cys199 and Tyr149. The FMN phosphate-binding loop (Thr94-Leu95-Gly96-Gly97-Ser98-Thr99) conforms to the phosphate binding Pi-loop consensus motif T/S-X-T-G-X-T (Drennan *et al.*, 1999), except for the glycine in the third position. In addition, the Gly97 carbonyl makes polar contact with the Lys101 amide. Lys101, Lys226, and Lys229 flank a ~8 Å-wide entry point to FMN- binding site, which might be relevant FMN binding, and, in the context of the full length Tyw1, for access to tRNA[Phe] m^1G37 and pyruvate.

Diametrically opposite the FMN binding site there is a system of several loops (Figure 1B Left), the longest of which (residues 168-180) contains Asp168-Phe169-Arg170 and Leu176, residues conserved in all TYW1 proteins (Extended Data Figure 2). This loop is the most structurally dissimilar from the nearest structural homologues identified by a DALI search: eukaryotic NADP(H)-cytochrome 450 diflavin oxidoreductase (3QFC) and nitric-oxide synthase (1TLL), and bacterial flavodoxin (5LJI) and sulfite reductase NADP(H) flavoprotein (1YKG) (Extended Data Figure 2). The unexpected anomalous feature present in our Tyw1 76-251 crystals, which is within coordination distance of Asp128, Asp130 and Glu131, was modeled as two Mn^{+2} ions bridged by a water molecule (Figure 1B Right) based on the strength and shape of the anomalous signal, the coordination geometry of the observed binding site, and manganese bioavailability in the expression host. The absence of these bound Mn^{+2} ions in our Tyw1 30-251 crystals might be due to use of a different recombinant tag, occlusion of the binding site by the flexible amino-terminal extension Tyw1 30-80, different crystallization conditions.

In summary, our experimental observations prove that *Schizosaccharomyces japonicus* Tyw1 has a stable, flavodoxin-like domain capable of recognizing FMN. Flavodoxin-like domains are found in proteins that function in electron transport

systems (oxidoreductases, transferases, lyases, isomerases, and ligases) and the presence of a possible functional metal ion-binding site in Tyw1 flavodoxin-like domain, together with binding of an iron-sulfur cluster in the Tyw1 carboxyl terminal domain, might contribute to Tyw1 functions. Structural similarity of its flavodoxin-like domain to those of enzymes that couple NADP(H) and FAD/FMN for their activity suggests regulation of Tyw1 by the cellular redox state. The interplay of flavin and NADH/NADPH in TYW1 proteins was also noted by Young and Bandarian (Young and Bandarian, 2021) after the atomic coordinates for our structures were released. These results will help further elucidation of the structural enzymology of 4-demethylwyosine synthesis in eukaryotes.

Methods

Schizosaccharomyces japonicus yFS275/FY16936 *tyw1* fragments encompassing Tyw1 residues 30-251 and 76-251 were cloned in bacterial expression vectors conferring N-terminal TRX-6His or MBP-6His tags and a TEV site. Cloning details are summarized in Extended Data Table 1. Transformed *Escherichia coli* KRX (Promega) were grown in Terrific Broth medium supplemented with 100 µg l^{-1} ampicillin at 310 K until OD$_{600}$ ~ 0.6 and recombinant protein expression was induced with 1 mM IPTG and 0.2 % rhamnose for 12 hr at 291 K. Cells were lysed in 0.5 M NaCl, 20 mM imidazole, 5% glycerol, 50 mM Hepes-NaOH pH 7.8, 0.5 mM 2-mercaptoethanol (LyB buffer) containing 1 mM PMSF. Recombinant proteins were applied on nickel nitrilotriacetic acid affinity (NiNTA) resin (Qiagen) and eluted in LyB supplemented with 330 mM imidazole, exchanged in LyB on 10 kDa cut-off concentrator (PALL Corporation) and digested with 6His-tagged TEV, passed again over NiNTA, concentrated, and loaded on HiLoad Superdex 75 pg 16/60 column (GE Healthcare) in 0.5 M KCl, 20 mM NaCl, 5% glycerol, 2 mM MgCl$_2$, 50 mM Hepes-KOH 7.5, 0.5 mM 2- mercaptoethanol, and exchanged into 150 mM KCl, 20 mM NaCl, 2 mM MgCl$_2$, 5% glycerol, 50 mM Hepes-NaOH pH 7.5, 0.5 mM 2-mercaptoethanol (AUC buffer). Analytical ultracentrifugation was performed in AUC buffer, at 293 K, absorbance was measured at 280 nm, run speed was 60,000 RPM, and the reference cell contained AUC buffer. Data were analyzed using SEDFIT (Schuck and Rossmanith, 2000), assuming a partial specific volume of 0.73 cm^3 g^{-1} and hydration value of 0.3.

S. japonicus Tyw1 constructs were crystallized by vapor diffusion. Hanging drops were prepared by mixing 200 nl of protein and 100 nl of reservoir solution using a Mosquito robot (TTP LabTech) and equilibrated against 100 µl of reservoir solution. *S. japonicus* Tyw1 76-251 (concentrated to ~38 g l^{-1}) crystallized as yellow tetragonal prisms at 295 K using a reservoir solution comprised of 100 mM Hepes-NaOH pH 7.5, 100 mM MOPS pH 7.5, 9.4% (v/v) MPD, 9.4% (v/v) PEG1000, 9.4% (w/v) PEG 3350, 300 mM MgCl$_2$, and 300 mM CaCl$_2$. Crystallization details are summarized in Extended Data Table 2. Crystals grew to maximal dimensions of 150 x 50 x 50 µm^3 in 10 days. *S. japonicus* Tyw1 30-251 (concentrated to ~12 g l^{-1}) crystallized as yellow tetragonal pyramids crystals at 288 K using a reservoir solution comprised of 200 mM sodium acetate, 30% (w/v) PEG 4000, 100 mM Tris- HCl pH 8.5. Crystals grew to maximum dimensions of 300 x 300 x 300 µm^3 within two weeks. Crystals were transferred to their respective reservoir solutions supplemented with 20% (v/v) PEG 400, mounted in nylon loops, and flash-frozen by plunging into liquid nitrogen. After exposure to X- rays, crystals were still yellow, and no color alteration was visible.

Diffraction data were collected at 100 K in rotation mode at beam lines 5.0.1 and 5.0.2 of the Advanced Light Source, Lawrence Berkeley National Laboratory (ALS) using 1.0 Å X-radiation, and integrated and scaled with DIALS (Winter *et al*., 2018). Data collection and processing statistics are summarized in Extended Data Table 3.

The Tyw1 76-251 (PDB 6PUP) structure was solved by single-wavelength anomalous dispersion (SAD) and automatically built using the Crank2 pipeline implemented in ccp4i2 (Skubak *et al*., 2018; Potterton *et al*., 2018). The mean overall figure of merit prior to density modification was 0.148. The model was manually rebuilt (Emsley and Cowtan, 2004) and was refined using Refmac5 (Murshudov *et al*., 2011). The final refinement statistics are summarized in Extended Data Table 4. Although the identity of the anomalous scatterer in the Tyw1 76-251 fragment is not certain (see below), it was modeled as a binuclear, water bridged Mn^{+2} complex, based on anomalous scattering, B-factor and geometric analysis. Tyw1 30-251 data did not exhibit anomalous signal, and its structure (PDB 6PUQ) was determined by molecular replacement (McCoy *et al*., 2007) using the Tyw1 76-251 structure (6PUP) as search model. The top solution had LLG and TFZ scores of 960 and 28.8, respectively. The model was refined using Phenix-Refine (Adams *et al*., 2010) (Extended Data Table 4). FMN density was strong and was modeled with unit occupancy in both structures. Structural figures were generated with PyMol (DeLano, 2002).

Reagents

Schizosaccharomyces japonicus tyw1 Uniprot B6K6D6_SCHJY strain yFS275/FY16936 synthetic gene

Proteopedia Molecular Tour

Extended Data

Description: Cartoon and molecular surface representations of the Tyw1 76-251 structure; Sequence alignment of TYW1 proteins; FMN binding site in S. japonicus Tyw1 30-251 crystal structure; Crystallization, data collection and processing, structure refinement details. Resource Type: Text. File: Extended Data flavodoxin-like domain Tyw1.docx. DOI: 10.22002/D1.20189

References

Cacoub P, Wechsler B, Chapelon C, Thibon M, Godeau P. 1991. Q-fever endocarditis and treatment with the fluoroquinolones. Arch Intern Med 151: 816, 818. PubMed ID: 2012470

Björk GR, Jacobsson K, Nilsson K, Johansson MJ, Byström AS, Persson OP. 2001. A primordial tRNA modification required for the evolution of life? EMBO J 20: 231-9. PubMed ID: 11226173

Carlson BA, Kwon SY, Chamorro M, Oroszlan S, Hatfield DL, Lee BJ. 1999. Transfer RNA modification status influences retroviral ribosomal frameshifting. Virology 255: 2-8. PubMed ID: 10049815

Droogmans L, Grosjean H. 1987. Enzymatic conversion of guanosine 3' adjacent to the anticodon of yeast tRNAPhe to N1-methylguanosine and the wye nucleoside: dependence on the anticodon sequence. EMBO J 6: 477-83. PubMed ID: 3556165

Grell TAJ, Young AP, Drennan CL, Bandarian V. 2018. Biochemical and Structural Characterization of a Schiff Base in the Radical-Mediated Biosynthesis of 4-Demethylwyosine by TYW1. J Am Chem Soc 140: 6842-6852. PubMed ID: 29792696

Hatfield D, Feng YX, Lee BJ, Rein A, Levin JG, Oroszlan S. 1989. Chromatographic analysis of the aminoacyl-tRNAs which are required for translation of codons at and around the ribosomal frameshift sites of HIV, HTLV-1, and BLV. Virology 173: 736-42. PubMed ID: 2556852

Helm M, Alfonzo JD. 2014. Posttranscriptional RNA Modifications: playing metabolic games in a cell's chemical Legoland. Chem Biol 21: 174-85. PubMed ID: 24315934

Huh WK, Falvo JV, Gerke LC, Carroll AS, Howson RW, Weissman JS, O'Shea EK. 2003. Global analysis of protein localization in budding yeast. Nature 425: 686-91. PubMed ID: 14562095

Krauss G, Peters F, Maass G. 1976. Effect of excision of the Y-base on the interaction of tRNAPhe (yeast) with phenylalanyl-tRNA synthetase (yeast). Nucleic Acids Res 3: 631-9. PubMed ID: 5707

Kumar KSD, Gurusaran M, Satheesh SN, Radha P, Pavithra S, Thulaa Tharshan KPS, Helliwell JR, Sekar K. 2015. Online_DPI: a web server to calculate the diffraction precision index for a protein structure. J Appl Cryst 48, 939-942. DOI: 10.1107/S1600576715006287

Li L, Miao R, Bertram S, Jia X, Ward DM, Kaplan J. 2012. A role for iron-sulfur clusters in the regulation of transcription factor Yap5-dependent high iron transcriptional responses in yeast. J Biol Chem 287: 35709-35721. PubMed ID: 22915593

Murshudov GN; Skubák P; Lebedev AA; Pannu NS; Steiner RA; Nicholls RA; et al.; Vagin AA. 2011. REFMAC5 for the refinement of macromolecular crystal structures. Acta Crystallogr D Biol Crystallogr 67: 355-67. PubMed ID: 21460454

Noma A, Kirino Y, Ikeuchi Y, Suzuki T. 2006. Biosynthesis of wybutosine, a hyper-modified nucleoside in eukaryotic phenylalanine tRNA. EMBO J 25: 2142-54. PubMed ID: 16642040

Potterton L; Agirre J; Ballard C; Cowtan K; Dodson E; Evans PR; et al.; Wojdyr M. 2018. CCP4i2: the new graphical user interface to the CCP4 program suite. Acta Crystallogr D Struct Biol 74: 68-84. PubMed ID: 29533233

Robert X, Gouet P. 2014. Deciphering key features in protein structures with the new ENDscript server. Nucleic Acids Res 42: W320-4. PubMed ID: 24753421

Schuck P, Rossmanith P. 2000. Determination of the sedimentation coefficient distribution by least-squares boundary modeling. Biopolymers 54: 328-41. PubMed ID: 10935973

Skubák P; Araç D; Bowler MW; Correia AR; Hoelz A; Larsen S; et al.; Pannu NS. 2018. A new MR-SAD algorithm for the automatic building of protein models from low-resolution X-ray data and a poor starting model. IUCrJ 5: 166-171. PubMed

ID: [29765606](#)

Young AP, Bandarian V. 2011. Pyruvate is the source of the two carbons that are required for formation of the imidazoline ring of 4-demethylwyosine. Biochemistry 50: 10573-5. PubMed ID: [22026549](#)

Young AP, Bandarian V. 2015. Mechanistic Studies of the Radical S-Adenosyl-L-methionine Enzyme 4-Demethylwyosine Synthase Reveal the Site of Hydrogen Atom Abstraction. Biochemistry 54: 3569-72. PubMed ID: [26052987](#)

Young AP, Bandarian V. 2021. Eukaryotic TYW1 Is a Radical SAM Flavoenzyme. Biochemistry 60: 2179-2185. PubMed ID: [34184886](#)

Ruan B; Nakano H; Tanaka M; Mills JA; DeVito JA; Min B; et al.; Söll D. 2004. Cysteinyl-tRNA(Cys) formation in Methanocaldococcus jannaschii: the mechanism is still unknown. J Bacteriol 186: 8-14. PubMed ID: [14679218](#)

Winter G; Waterman DG; Parkhurst JM; Brewster AS; Gildea RJ; Gerstel M; et al.; Evans G. 2018. DIALS: implementation and evaluation of a new integration package. Acta Crystallogr D Struct Biol 74: 85-97. PubMed ID: [29533234](#)

Zheng H, Cooper DR, Porebski PJ, Shabalin IG, Handing KB, Minor W. 2017. CheckMyMetal: a macromolecular metal-binding validation tool. Acta Crystallogr D Struct Biol 73: 223-233. PubMed ID: [28291757](#)

Author Contributions: Ljiljana Sjekloća: conceptualization, data curation, validation, visualization, writing - original draft, writing - review editing. Adrian R. Ferré-D'Amaré: supervision, resources, validation, writing - original draft, funding acquisition.

Reviewed By: Joel Sussman

Citation: Sjekloća, L; Ferré-D'Amaré, AR (2022). Biochemical and structural characterization of the flavodoxin-like domain of the *Schizosaccharomyces japonicus* putative tRNA[Phe] 4-demethylwyosine synthase Tyw1 in complex with FMN. microPublication Biology. [10.17912/micropub.biology.000570](#)